Original Article

Ultrasound diagnosis of parathyroid adenomas mimicking normal lymph nodes: microvascular clues

Song Fang[1], Qingli Zhu[1], Jialin Zhao[1], Xiaoyan Chang[2], Quan Liao[3], Ou Wang[4], Xiaoping Xing[4], Jianchu Li[1], He Liu[1]

[1]Department of Ultrasound, Peking Union Medical College Hospital, Chinese Academy of Medical Sciences and Peking Union Medical College, Beijing, China; [2]Department of Pathology, Peking Union Medical College Hospital, Chinese Academy of Medical Sciences and Peking Union Medical College, Beijing, China; [3]Department of General Surgery, Peking Union Medical College Hospital, Chinese Academy of Medical Sciences and Peking Union Medical College, Beijing, China; [4]Department of Endocrinology, Peking Union Medical College Hospital, Chinese Academy of Medical Sciences and Peking Union Medical College, Beijing, China

Contributions: (I) Conception and design: J Li, H Liu, S Fang; (II) Administrative support: J Li, H Liu; (III) Provision of study materials or patients: All authors; (IV) Collection and assembly of data: S Fang, H Liu, Q Zhu; (V) Data analysis and interpretation: S Fang, H Liu, J Zhao; (VI) Manuscript writing: All authors; (VII) Final approval of manuscript: All authors.

Correspondence to: Jianchu Li, MD; He Liu, MD. Department of Ultrasound, Peking Union Medical College Hospital, Chinese Academy of Medical Sciences and Peking Union Medical College, 1 Shuaifuyuan Street, Dongcheng District, Beijing 100730, China. Email: jianchuli_0301@163.com; liuhebj@126.com.

Background: Ultrasound (US) is the preferred imaging modality for preoperative localization of primary hyperparathyroidism (PHPT). Parathyroid adenomas may be confused with normal lymph nodes on conventional US. This study aimed to explore the usefulness of microvascular flow imaging (MVFI) in differentiating parathyroid adenomas from normal lymph nodes and compare it with color Doppler flow imaging (CDFI).

Methods: A total of 34 parathyroid adenomas that appeared peripherally hypoechoic and internally hyperechoic mimicking normal lymph nodes were identified in 34 patients with PHPT, and 34 cervical level III normal lymph nodes from 34 healthy controls were selected for comparison. The ability of CDFI and MVFI to detect the vascular characteristics of parathyroid adenomas were compared.

Results: On CDFI, the detection rates of polar vessels, hilar vessels, and rich vascular in parathyroid adenomas were 44.1%, 8.8%, and 52.9%, respectively. These characteristics in normal lymph nodes showed detection rates of 2.9%, 38.2%, and 8.8%, respectively. On MVFI, the detection rates of polar vessels, hilar vessels, and rich vascular in parathyroid adenomas were 82.4%, 5.9%, and 94.1%, respectively. For normal lymph nodes, the detection rates of these characteristics were 5.9%, 76.5%, and 11.8%, respectively. Compared with CDFI, MVFI detected a significantly higher rate of polar vessels and rich vascularity in parathyroid adenomas (82.4% *vs.* 44.1% and 94.1% *vs.* 52.9%, P=0.034 and P<0.001), as well as hilar vessels in normal lymph nodes (76.5% *vs.* 38.2%, P<0.001).

Conclusions: MVFI more frequently identified polar vessels and rich vascularity in parathyroid adenomas, as well as hilar vessels in lymph nodes, compared to CDFI. This suggests that MVFI may play a better role in differentiating parathyroid adenomas from lymph nodes, contributing to surgical planning in PHPT cases.

Keywords: Hyperparathyroidism; primary; color Doppler flow imaging (CDFI); microvascular flow imaging (MVFI)

Submitted Sep 26, 2024. Accepted for publication Jan 07, 2025. Published online Feb 12, 2025.
doi: 10.21037/qims-24-2057
View this article at: https://dx.doi.org/10.21037/qims-24-2057

Introduction

Primary hyperparathyroidism (PHPT) is a common endocrine disorder caused by pathological hypersecretion of parathyroid hormone (PTH) from one or more parathyroid glands (1,2). Parathyroid adenoma is the main cause of PHPT, contributing to approximately 80% of PHPT cases (3). Surgical excision of the abnormal parathyroid tissue is the only curative treatment for patients with PHPT. Accurate preoperative localization of parathyroid lesions is critical for a successful parathyroidectomy (4).

Ultrasound (US) is the preferred imaging modality for preoperative localization of PHPT, yielding a sensitivity of 49–89% (5-8). The typical sonographic appearance of a parathyroid adenoma on gray-scale imaging is an ovoid shape with a homogeneously hypoechoic shape compared to the adjacent thyroid tissue (9). However, some adenomas appear peripherally hypoechoic with internally hyperechoic areas, mimicking lymph nodes, and may be misdiagnosed (10,11). Previous studies have pointed out that parathyroid adenomas and lymph nodes exhibit different vascular patterns and may help in the differential diagnosis. Parathyroid adenomas are typically hypervascular, with a polar feeding vessel entering from the pole along the long axis (6,12,13). Lymph nodes are characterized by the hilar vessel, with branching vascular pedicles located centrally in the hilum (14). Conventional color Doppler flow imaging (CDFI) is a widely used US technique to evaluate the vascular pattern indirectly. It can depict vascular flow larger than 200 μm in diameter, but cannot show smaller vessels and slower capillary blood (<200 μm in diameter). Parathyroid lesions are usually small in size and located on the dorsal side of the thyroid lobes; their small size and relatively deep location interfere with the sensitivity of CDFI (15).

A novel Doppler technique, microvascular flow imaging (MVFI), may help resolve this problem. MVFI relies on a combination of approaches to reduce noise and separate low-velocity or small-vessel flow signals from clutter and slow-motion artifacts, without injecting contrast agents. It can improve the sensitivity to slow-flow Doppler signals and characterize vascular morphological details (16,17). At present, most high-end US systems are equipped with MVFI techniques, such as Superb microvascular imaging (Canon Medical Systems, Tokyo, Japan), AngioPLUS (SuperSonic Imagine, Aix-en-Provence, France), MicroFlow imaging (Philips Healthcare, Best, the Netherlands), and MV-Flow (Samsung Medison, Seoul, Korea). This study aimed to explore the usefulness of MVFI in differentiating parathyroid adenomas from lymph nodes and compare it with CDFI. We present this article in accordance with the STROBE reporting checklist (available at https://qims.amegroups.com/article/view/10.21037/qims-24-2057/rc).

Methods

Study participants

A total of 34 patients with PHPT and 34 healthy controls participated in this study. For inclusion in the PHPT patient group, individuals had to fulfill the following criteria: (I) diagnosed with PHPT according to the Diagnosis and Management of PHPT by the American Medical Association (18); (II) underwent US and MVFI assessments; (III) exhibited parathyroid lesions presenting as peripheral hypoechogenicity with internal hyperechogenicity, mimicking lymph nodes (*Figure 1A*) on gray-scale US; and (IV) underwent surgical treatments for PHPT with histopathological results available. All patients were consecutively recruited at Peking Union Medical College Hospital between March 2022 and July 2023. A total of 34 volunteers with no known underlying diseases were recruited as controls. Patients and healthy controls were matched for age (±3 years) and sex. This study was approved by the Ethics Committee of Peking Union Medical College Hospital (No. I-22PJ066) and conducted in accordance with the Declaration of Helsinki (as revised in 2013). All the participants provided written informed consent before participating in the study.

US and MVFI image acquisition

All US examinations were performed by a radiologist with more than 15 years of experience in superficial organs. The US machine used was Aplio i900 (Canon Medical Systems) or Aixplorer (SuperSonic Imagine) with linear array transducer (5–14 or 4–15 MHz) and preset condition of "thyroid". The patients were examined bilaterally from the mandible to the supraclavicular fossa. When abnormal echoes were detected, their location, size, echogenicity, long diameter/short diameter (L/S) ratio, and vascular characteristics were recorded. Cervical lymph nodes of level III (19) were scanned in healthy controls, selecting lymph nodes exhibiting peripheral hypoechogenicity with internal hyperechogenicity. We recorded their size and vascular characteristics.

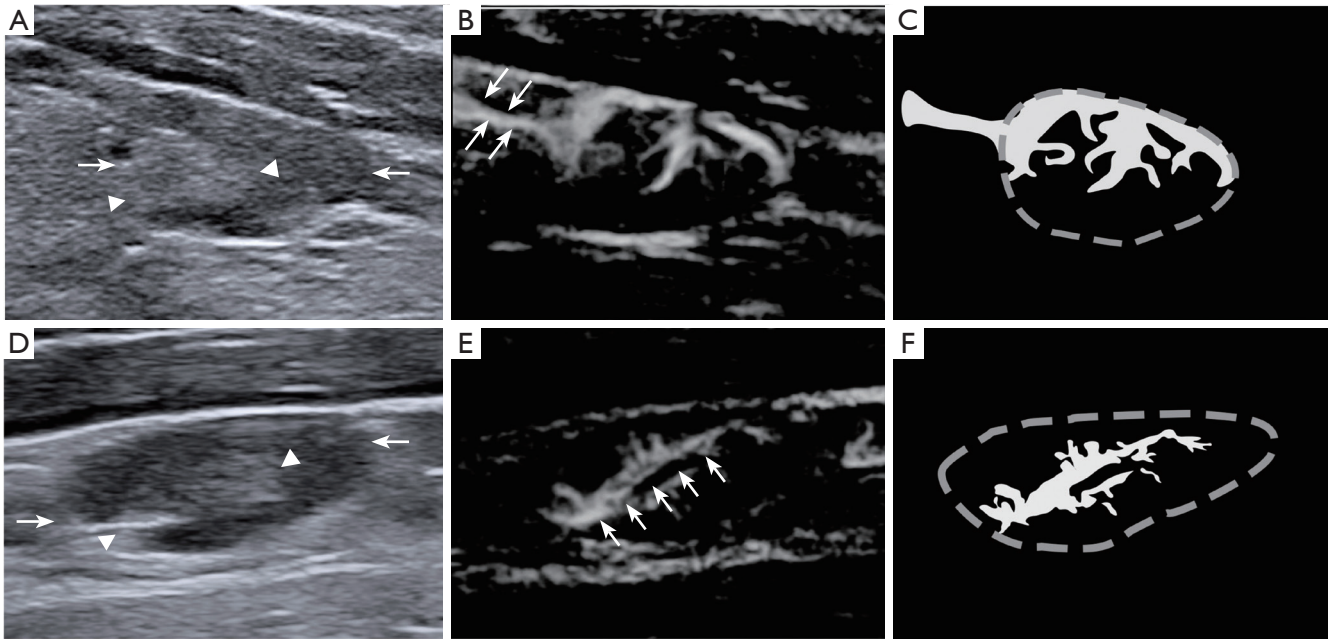

Figure 1 MVFI characteristics of parathyroid adenoma and normal cervical lymph. (A) Gray-scale US imaging of a parathyroid adenoma (arrows) with peripheral hypoechogenicity and internal hyperechogenicity (arrowheads). (B) MVFI shows the polar vessel (arrows) of the adenoma and rich vascularity with the division of multiple small vessels. (D) Gray-scale US imaging of a normal cervical lymph node (arrows) with peripheral hypoechogenicity and internal hyperechogenicity (arrowheads). (E) MVFI shows the hilar vessel (arrows) of the lymph node with the division of multiple small vessels. MVFI schematic diagrams of parathyroid adenoma (C) and normal cervical lymph node (F). MVFI, microvascular flow imaging; US, ultrasound.

Vascular characteristics were detected using CDFI and MVFI. MVFI image was obtained using Superb microvascular imaging (Canon Medical Systems) or AngioPLUS (SuperSonic Imagine). The parameters were as follows: velocity scale, <2 cm/s; frame rate, 25–45 frames/s; depth, 2–5 cm; imaging gain, 50–70%; dynamic range, 50–65 dB; and frequency, 5–14 MHz. All static and dynamic images were acquired and stored on the workstation for subsequent analyses.

CDFI and MVFI image analysis

Polar vessels (visible or invisible), hilar vessels (visible or invisible), and vascularity amount (rich, medium, or none) were assessed on the CDFI and MVFI images by a radiologist with more than 5 years of experience in superficial US. The polar vessel was defined as a feeding vessel terminating in the parathyroid adenoma, representing an enlarged feeding artery, and arborizing around the periphery (20,21). The hilar vessel was a branching vascular pedicle located centrally in the hilum (14). The vascularity amount was determined to be rich (≥3 vessels), medium (1–2 vessels), and none, based on Adler blood flow grading (22). To assess inter-observer reproducibility, another independent radiologist with more than 10 years of experience in superficial US was blinded to the clinical data reviewed the saved images, and repeated all the evaluations.

Surgery and histopathologic diagnosis

Surgeries were performed after the completion of the necessary examinations. An experienced parathyroid pathologist performed histopathological diagnosis of all lesions according to the World Health Organization (WHO) classification criteria (23).

Statistical analysis

Statistical analyses were performed using the software SPSS 26.0 (IBM Corp., Armonk, NY, USA). The normality

Table 1 Baseline characteristics of enrolled participants

Characteristics	PHPT patients (n=34)	Healthy controls (n=34)	P value
Male	7 (20.6)	7 (20.6)	>0.99
Age (years)	50.7±13.4	49.0±13.1	0.826
Clinical symptoms		–	–
Urinary symptoms	14 (41.2)		
Skeletal symptoms	8 (23.5)		
Gastrointestinal symptoms	2 (5.9)		
Neuromuscular symptoms	2 (5.9)		
Asymptomatic	8 (23.5)		
Serum PTH level (pg/mL)	140.5 (105.3–166.5)	–	–
Serum calcium level (mmol/L)	2.70±0.27	–	–
Concurrent thyroid disease		–	–
Yes	11 (32.4)		
No	23 (67.6)		
Previous neck surgery		–	–
Yes	6 (17.6)		
No	28 (82.4)		

Data are expressed as n (%), mean ± SD, or median (interquartile ranges). PHPT, primary hyperparathyroidism; PTH, parathyroid hormone; SD, standard deviation.

of the distribution of quantitative variables was tested using the Shapiro-Wilk test. Parametric data (age, serum calcium level, and size) are expressed as mean ± SD and was compared using independent samples Student's *t*-test. Non-parametric data (serum PTH level) are shown as medians with interquartile ranges and were compared using the Mann-Whitney *U* test. Categorical variables are shown as percentages and compared using Pearson's Chi-squared and Fisher's exact tests.

Intra- and inter-observer reproducibility was assessed by calculating the intra-class correlation coefficient (ICC) which was graded as follows: poor (<0.20), fair (0.20–0.40), moderate (0.41–0.60), good (0.61–0.80), or very good (0.81–1.00). A P value less than 0.05 was considered statistically significant.

Results

Patient characteristics

This study recruited 34 patients with PHPT and 34 age- and sex-matched healthy controls. The baseline characteristics of all participants are shown in *Table 1*. In both groups, 20.6% (7/34) of the patients were male. The mean age was 50.7±13.4 years in the PHPT patient group and 49.0±13.1 years in the control group, with no statistical difference (P=0.826). A total of 26 (26/34, 76.5%) patients with PHPT had obvious clinical symptoms, including urinary (n=14), skeletal (n=8), gastrointestinal (n=2), and neuromuscular symptoms (n=2). The median serum PTH was 140.5 pg/mL, and the mean calcium level was 2.70 mmol/L. A total of 11 (11/34, 32.4%) patients had concurrent thyroid disease, and six (6/34, 17.6%) patients had previously undergone neck surgery. Finally, 34 parathyroid lesions were found in 34 patients, all of which were pathologically confirmed as parathyroid adenomas, and 34 normal cervical lymph nodes from 34 healthy controls were selected for comparison.

Gray-scale US characteristics between PHPT and control groups

On gray-scale US, the maximum diameter of the parathyroid adenomas ranged from 1.0 to 3.6 cm, which was not significantly different from that of the normal lymph nodes in healthy controls (1.60±0.42 *vs.* 1.61±0.41 cm, Student's *t*-test, P=0.821). A total of 29 (29/34, 85.3%) parathyroid adenomas and 31 (31/34, 91.2%) normal lymph nodes had an L/S ratio ≥2, with no significant difference between the two groups (Fisher's exact test, P=0.709). Both parathyroid adenomas and normal lymph nodes appeared peripherally hypoechogenic and internally hyperechogenic.

Comparison of vascular characteristics between PHPT and control groups

The comparison of vascular characteristics between PHPT and control groups is shown in *Table 2*. Polar vessels (*Figure 1A-1C*) were more commonly detected in parathyroid adenomas than in normal lymph nodes (44.1% *vs.* 2.9% and 82.4% *vs.* 5.9%, Fisher's exact test, P<0.001). Hilar vessels (*Figure 1D-1F*) were more frequently observed in lymph nodes than in parathyroid lesions (38.2% *vs.*

Table 2 Vascular characteristics of PHPT and control groups

Characteristics	CDFI			MVFI		
	PA (n=34)	LN (n=34)	P value	PA (n=34)	LN (n=34)	P value
Polar vessel	15 (44.1)	1 (2.9)	<0.001	28 (82.4)	2 (5.9)	<0.001
Hilar vessel	3 (8.8)	13 (38.2)	0.009	2 (5.9)	26 (76.5)	<0.001
Vascularity amount			<0.001			<0.001
Rich	18 (52.9)	3 (8.8)		32 (94.1)	4 (11.8)	
Medium	16 (47.1)	15 (44.1)		2 (5.9)	16 (47.1)	
None	0 (0)	16 (47.1)		0 (0)	14 (41.2)	

Qualitative data are expressed as n (%). PHPT, primary hyperparathyroidism; CDFI, color Doppler flow imaging; MVFI, microvascular flow imaging; PA, parathyroid adenoma; LN, lymph node.

Table 3 Comparison of CDFI and MVFI in the detection of vascularity of PHPT and control groups

Characteristics	PA			LN		
	CDFI (n=34)	MVFI (n=34)	P value	CDFI (n=34)	MVFI (n=34)	P value
Polar vessel	15 (44.1)	28 (82.4)	0.034	1 (2.9)	2 (5.9)	>0.99
Hilar vessel	3 (8.8)	2 (5.9)	>0.99	13 (38.2)	26 (76.5)	0.003
Vascularity amount			<0.001			0.857
Rich	18 (52.9)	32 (94.1)		3 (8.8)	4 (11.8)	
Medium	16 (47.1)	2 (5.9)		15 (44.1)	16 (47.1)	
None	0 (0)	0 (0)		16 (47.1)	14 (41.2)	

Qualitative data are expressed as n (%). CDFI, color Doppler flow imaging; MVFI, microvascular flow imaging; PA, parathyroid adenoma; LN, lymph node.

8.8% and 76.5% *vs.* 5.9%, Fisher's exact test, P=0.009 and P<0.001). Rich vascularity was observed more frequently in parathyroid adenomas than in lymph nodes (52.9% *vs.* 8.8% and 94.1% *vs.* 11.8%, Fisher's exact test, P<0.001).

Comparison of CDFI and MVFI in the detection of vascular characteristics of PHPT and control groups

The comparison of CDFI and MVFI in the detection of vascular characteristics of PHPT and control groups is shown in *Table 3*. Compared to CDFI, MVFI detected a significantly higher rate of polar vessels and rich vascularity in parathyroid adenomas (82.4% *vs.* 44.1% and 94.1% *vs.* 52.9% Fisher's exact test, P=0.034 and P<0.001) (*Figure 2A-2F*), as well as a significantly higher rate of hilar vessels in normal lymph nodes (76.5% *vs.* 38.2% Pearson's Chi-squared test, P<0.001) (*Figure 3A-3C*). CDFI and MVFI showed no significant differences in the detection of hilar vessels in parathyroid adenomas, as well as the detection of polar vessels and the vascularity amount in lymph nodes (Fisher's exact and Pearson's Chi-squared tests, P>0.99, P>0.99, and P=0.857).

Intra- and inter-observer reproducibility for CDFI and MVFI image analysis

For intra-observer reproducibility, the ICC of the polar vessel, hilar vessel, and vascularity amount on CDFI and MVFI ranged from 0.765 to 0.909. For inter-observer reproducibility, the ICC of the polar vessel, hilar vessel, and vascularity amount on CDFI and MVFI ranged from 0.688 to 0.880. These results indicate that vascular characteristics on CDFI and MVFI had good intra-observer and inter-observer reproducibility (*Table 4*).

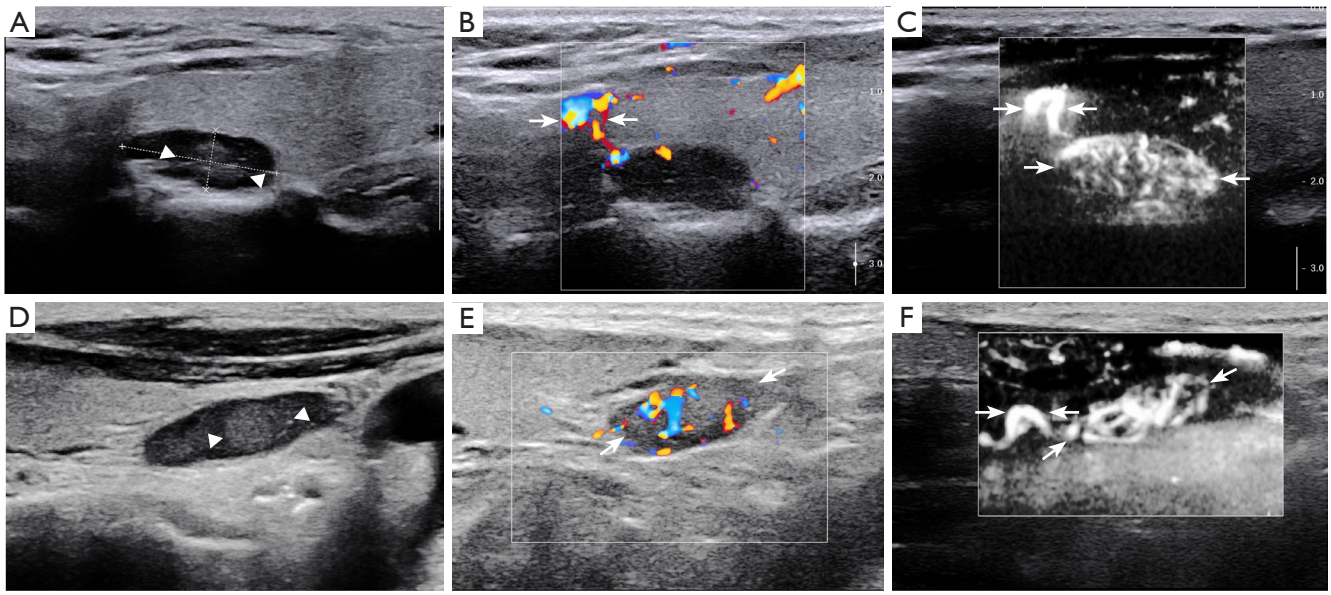

Figure 2 Vascular characteristics of parathyroid adenomas on CDFI and MVFI. (A-C) A right inferior parathyroid adenoma of a 29-year-old woman. (A) Gray-scale US shows the hypoechogenic parathyroid lesion with hyperechogenicity in the center (arrowheads). (B) CDFI shows the polar vessel (arrows) and medium vascularity. (C) MVFI shows the polar vessel and rich vascularity with the division of multiple small vessels (arrows). (D-F) A right inferior parathyroid adenoma of a 72-year-old man. (D) Gray-scale US shows the hypoechogenic parathyroid lesion with hyperechogenicity in the center (arrowheads). (E) CDFI shows rich vascularity (arrows). (F) MVFI shows the polar vessel and rich vascularity with the division of multiple small vessels (arrows). CDFI, color Doppler flow imaging; MVFI, microvascular flow imaging; US, ultrasound.

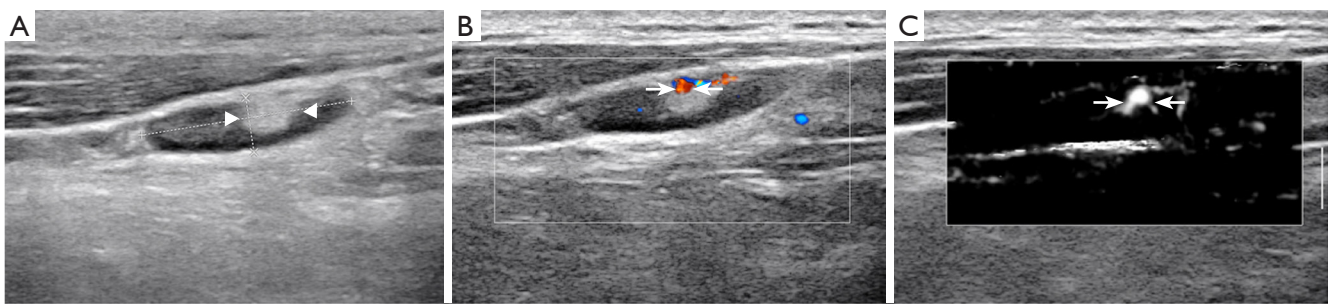

Figure 3 A normal cervical lymph node of a 72-year-old man. (A) Gray-scale US shows the lymph node with internal hyperechogenicity (arrowheads). (B) CDFI shows medium vascularity peripherally (arrows). (C) MVFI shows the hilar vessel with the division of multiple small vessels (arrows). US, ultrasound; CDFI, color Doppler flow imaging; MVFI, microvascular flow imaging.

Discussion

In this study, we used gray-scale US, CDFI, and MVFI to evaluate the US characteristics of 34 parathyroid adenomas mimicking normal lymph nodes, and compared them with 34 normal lymph nodes. Based on good to very good intra- and inter-observer reproducibility (ICC: 0.688–0.909) for CDFI and MVFI images, we found that polar vessels, rich vascularity, and the absence of hilar vessels were very useful characteristics for differentiating parathyroid adenomas from lymph nodes and that MVFI was a valuable tool for differential diagnosis. Compared with CDFI, MVFI showed a superior ability to detect the vascular characteristics of parathyroid adenomas.

Parathyroid adenomas typically appear ovoid and

Table 4 Intra-observer and inter-observer reproducibility for CDFI and MVFI image analysis

Characteristics	ICC (95% CI)	
	Intra-observer reproducibility	Inter-observer reproducibility
CDFI		
Polar vessel	0.769 (0.577–0.961)	0.731 (0.529–0.933)
Hilar vessel	0.765 (0.587–0.934)	0.688 (0.492–0.884)
Vascularity amount	0.817 (0.697–0.937)	0.841 (0.729–0.953)
MVFI		
Polar vessel	0.909 (0.809–1)	0.786 (0.639–0.933)
Hilar vessel	0.847 (0.718–0.976)	0.880 (0.766–0.994)
Vascularity amount	0.830 (0.712–0.948)	0.769 (0.622–0.916)

CDFI, color Doppler flow imaging; MVFI, microvascular flow imaging; ICC, intra-class correlation coefficient; CI, confidence interval.

homogeneously hypoechoic on gray-scale imaging (9). Normal lymph nodes typically appear peripherally hypoechogenic and internally hyperechogenic with an ovoid shape and an L/S ratio ≥2 (24,25). In this study, we selected 34 adenomas that showed peripherally hypoechogenic with internally hyperechogenic area. Among them, 85.3% had an L/S ratio ≥2, mimicking cervical lymph nodes, and were able to be misdiagnosed.

Recent studies have suggested that parathyroid adenomas mimicking normal lymph nodes on gray-scale US can be explained by histopathology. Acar *et al.* (10) observed the hyperechoic central zone with the peripherally hypoechoic layer in nine out of 56 parathyroid adenomas and called the novel characteristic "dual concentric echo sign". They evaluated the histopathological characteristics and demonstrated significantly increased edema (P<0.01) and ectatic vessels (P<0.02) in parathyroid adenomas with this characteristic compared with classic hypoechoic parathyroid adenomas. Li *et al.* (11) conducted further research on the histopathological components of the hypoechoic and hyperechoic areas of parathyroid adenomas. They observed 45 parathyroid adenomas, and the histopathological results revealed that the hypoechoic area had more cellular components (chief cells, oxophilic cells, and water-clear cells), whereas the hyperechoic area had more non-functional components, such as lipocytes, connective tissue, edematous tissue, and normal parathyroid tissue. Different from parathyroid adenoma, the lymph node is characterized by an outer hypoechoic cortex and an inner hyperechoic medulla. The hyperechoic medulla contains a dense network of lymphatic cords and sinuses. The numerous interfaces between these sinuses, many of which are perpendicular to the sonographic beam, make strong reflectors. Conversely, the homogeneous composition of lymphoid follicles within the cortex results in its hypoechoic appearance (24,25). Despite their completely different histopathological composition, this kind of parathyroid adenoma is difficult to differentiate from normal lymph nodes using gray-scale US. Investigators look for vascular clues to assist in distinction.

CDFI has been shown to be a valuable tool in the differential diagnosis of parathyroid adenomas and normal lymph nodes. The drawback is that it is sensitive only to vessels larger than about 200 μm in diameter (26,27). Useful clues, such as polar vessels and rich vascularity for parathyroid adenoma, as well as hilar vessels for lymph nodes, were only visible in approximately 44.6–60.2%, 39.6–51.8%, and 37.9–67.0% of cases, respectively (9,28-31). These results were similar to those of our study. Inclusive analysis of this and previous studies indicated that a significant proportion of parathyroid lesions (39.8–55.4%) and normal lymph nodes (48.2–62.1%) could not well show the polar vessels and hilar vessels on CDFI, providing limited diagnostic information. Seeking a more sensitive Doppler technique to effectively differentiate parathyroid adenomas from normal lymph nodes is crucial.

In this study, MVFI detected polar vessels and rich vascularity in 82.4% and 94.1% of parathyroid adenomas, respectively, which were higher than those of CDFI (38.2%). These results are consistent with previous studies. A previous study using MVFI to analyze 30 parathyroid lesions also showed that, when compared to CDFI, MVFI significantly improved the visualization of polar vessels (53.3% *vs.* 20.0%) and the peripheral/internal blood flow (83.3% *vs.* 50.0%) in these lesions (21). This study included 34 parathyroid lesions, more than in previous studies, and compared parathyroid lesions with 34 normal lymph nodes. We not only observed the microvascular characteristics of parathyroid adenomas but also evaluated the usefulness of MVFI in the differential diagnosis of parathyroid adenomas and lymph nodes. According to the results of this study, MVFI is a useful tool for differentiating parathyroid adenomas from lymph nodes. Compared with CDFI, MVFI may assist in the detection of vascular characteristics of parathyroid adenomas.

Evaluation of polar vessels in parathyroid adenomas using MVFI should be integrated with gray-scale US and

CDFI. The majority of parathyroid glands receive blood supply from the superior or inferior thyroid artery, with some receiving blood supply from both. These arteries terminate in the parathyroid adenomas and branch off into the adenomas (32-34). On US, these arteries are referred to as polar vessels. In this study, polar vessels were observed in 28 parathyroid adenomas using MVFI. In contrast to normal lymph nodes, where blood supply arteries enter the hyperechoic medulla, 25 of the 28 parathyroid adenomas exhibited blood supply arteries entering from the hypoechoic area and branching within the adenoma. The integration of gray-scale US and MVFI provides significant value in the differential diagnosis of parathyroid adenomas and normal lymph nodes. Most current MVFI techniques, such as Superb microvascular imaging (Canon Medical Systems), MicroFlow imaging (Philips Healthcare), and MV-Flow (Samsung Medison), cannot visualize the blood flow direction. Visualizing the blood flow direction is important for identifying the polar vessels of parathyroid lesions, as large draining veins of parathyroid lesions may sometimes be mistaken for polar vessels. CDFI can visualize the blood flow direction and help differentiate them. Some MVFI techniques, such as AngioPLUS (SuperSonic Imagine), have been upgraded to visualize blood flow direction (35). With further technological development, we believe that MVFI may replace CDFI if the visualization of blood flow direction in MVFI becomes widespread.

MVFI can observe microvessels in real-time and provide more useful information for diagnosis (16). Consequently, when using MVFI to perform parathyroid US examination, the machine should be adjusted to appropriate parameters. When evaluating superficial suspicious lesions, it is advisable to minimize probe pressure, integrate gray-scale US, and perform a comprehensive evaluation to obtain more accurate diagnostic information.

Our study had some limitations. First, this was a preliminary study conducted in a single center, and the sample size was small, which may have caused a potential selection bias. Second, although we evaluated the value of MVFI characteristics in the differentiation of parathyroid adenoma from lymph nodes, the diagnostic performance, such as the sensitivity and accuracy of MVFI, was not studied. Third, the pathological basis of parathyroid adenomas mimicking lymph nodes was not fully evaluated.

Conclusions

In our sample, MVFI more frequently identified polar vessels and rich vascularity in parathyroid adenomas, as well as hilar vessels in lymph nodes, compared to CDFI. It also demonstrated good intra- and inter-observer reproducibility. This suggests that MVFI may play a better role in differentiating parathyroid adenomas from lymph nodes, contributing to surgical planning in PHPT cases. Further studies in larger and diverse populations are needed to better evaluate this technique.

Acknowledgments

None.

Footnote

Reporting Checklist: The authors have completed the STROBE reporting checklist. Available at https://qims.amegroups.com/article/view/10.21037/qims-24-2057/rc

Funding: This work was supported by the National High Level Hospital Clinical Research Funding (grant Nos. 2022-PUMCH-B-065 and 2022-PUMCH-B-064).

Conflicts of Interest: All authors have completed the ICMJE uniform disclosure form (available at https://qims.amegroups.com/article/view/10.21037/qims-24-2057/coif). All authors report that this work was supported by the National High Level Hospital Clinical Research Funding (grant Nos. 2022-PUMCH-B-065 and 2022-PUMCH-B-064). The authors have no other conflicts of interest to declare.

Ethical Statement: The authors are accountable for all aspects of the work in ensuring that questions related to the accuracy or integrity of any part of the work are appropriately investigated and resolved. This study was approved by the Ethics Committee of Peking Union Medical College Hospital (No. I-22PJ066) and conducted in accordance with the Declaration of Helsinki (as revised in 2013). All the participants provided written informed consent before participating in the study.

References

1. Bilezikian JP, Bandeira L, Khan A, Cusano NE. Hyperparathyroidism. Lancet 2018;391:168-78.
2. Walker MD, Silverberg SJ. Primary hyperparathyroidism. Nat Rev Endocrinol 2018;14:115-25.
3. Udelsman R. Six hundred fifty-six consecutive explorations for primary hyperparathyroidism. Ann Surg 2002;235:665-70; discussion 670-2.
4. Wilhelm SM, Wang TS, Ruan DT, Lee JA, Asa SL, Duh QY, Doherty GM, Herrera MF, Pasieka JL, Perrier ND, Silverberg SJ, Solórzano CC, Sturgeon C, Tublin ME, Udelsman R, Carty SE. The American Association of Endocrine Surgeons Guidelines for Definitive Management of Primary Hyperparathyroidism. JAMA Surg 2016;151:959-68.
5. Chandramohan A, Sathyakumar K, Irodi A, Abraham D, Paul MJ. Causes of discordant or negative ultrasound of parathyroid glands in treatment naïve patients with primary hyperparathyroidism. Eur J Radiol 2012;81:3956-64.
6. Bunch PM, Kelly HR. Preoperative Imaging Techniques in Primary Hyperparathyroidism: A Review. JAMA Otolaryngol Head Neck Surg 2018;144:929-37.
7. Iwen KA, Kußmann J, Fendrich V, Lindner K, Zahn A. Accuracy of Parathyroid Adenoma Localization by Preoperative Ultrasound and Sestamibi in 1089 Patients with Primary Hyperparathyroidism. World J Surg 2022;46:2197-205.
8. Park HS, Hong N, Jeong JJ, Yun M, Rhee Y. Update on Preoperative Parathyroid Localization in Primary Hyperparathyroidism. Endocrinol Metab (Seoul) 2022;37:744-55.
9. Lane MJ, Desser TS, Weigel RJ, Jeffrey RB Jr. Use of color and power Doppler sonography to identify feeding arteries associated with parathyroid adenomas. AJR Am J Roentgenol 1998;171:819-23.
10. Acar T, Ozbek SS, Ertan Y, Kavukcu G, Tuncyurek M, Icoz RG, Akyildiz MM, Makay O, Acar S. Variable sonographic spectrum of parathyroid adenoma with a novel ultrasound finding: dual concentric echo sign. Med Ultrason 2015;17:139-46.
11. Li J, Yang X, Chang X, Ouyang Y, Hu Y, Li M, Xiao M, Gui Y, Chen X, Tan L, Hao F, Li J, Lv K, Jiang Y. A Retrospective Study of Ultrasonography in the Investigation of Primary Hyperparathyroidism: A New Perspective for Ultrasound Echogenicity Features of Parathyroid Nodules. Endocr Pract 2021;27:1004-10.
12. Reeder SB, Desser TS, Weigel RJ, Jeffrey RB. Sonography in primary hyperparathyroidism: review with emphasis on scanning technique. J Ultrasound Med 2002;21:539-52; quiz 553-4.
13. Centello R, Sesti F, Feola T, Sada V, Pandozzi C, Di Serafino M, Pacini P, Cantisani V, Giannetta E, Tarsitano MG. The Dark Side of Ultrasound Imaging in Parathyroid Disease. J Clin Med 2023;12:2487.
14. Jacobson JA, Middleton WD, Allison SJ, Dahiya N, Lee KS, Levine BD, Lucas DR, Murphey MD, Nazarian LN, Siegel GW, Wagner JM. Ultrasonography of Superficial Soft-Tissue Masses: Society of Radiologists in Ultrasound Consensus Conference Statement. Radiology 2022;304:18-30.
15. Petranović Ovčariček P, Giovanella L, Carrió Gasset I, Hindié E, Huellner MW, Luster M, Piccardo A, Weber T, Talbot JN, Verburg FA. The EANM practice guidelines for parathyroid imaging. Eur J Nucl Med Mol Imaging 2021;48:2801-22.
16. Aziz MU, Eisenbrey JR, Deganello A, Zahid M, Sharbidre K, Sidhu P, Robbin ML. Microvascular Flow Imaging: A State-of-the-Art Review of Clinical Use and Promise. Radiology 2022;305:250-64.
17. Park AY, Kwon M, Woo OH, Cho KR, Park EK, Cha SH, Song SE, Lee JH, Cha J, Son GS, Seo BK. A Prospective Study on the Value of Ultrasound Microflow Assessment to Distinguish Malignant from Benign Solid Breast Masses: Association between Ultrasound Parameters and Histologic Microvessel Densities. Korean J Radiol 2019;20:759-72.
18. Zhu CY, Sturgeon C, Yeh MW. Diagnosis and Management of Primary Hyperparathyroidism. JAMA 2020;323:1186-7.
19. Robbins KT, Clayman G, Levine PA, Medina J, Sessions R, Shaha A, Som P, Wolf GT; . Neck dissection classification update: revisions proposed by the American Head and Neck Society and the American Academy of Otolaryngology-Head and Neck Surgery. Arch Otolaryngol Head Neck Surg 2002;128:751-8.
20. Kamaya A, Quon A, Jeffrey RB. Sonography of the abnormal parathyroid gland. Ultrasound Q 2006;22:253-62.
21. Liu H, Liao Q, Wang Y, Hu Y, Zhu Q, Wang L, Liu Q, Li J, Jiang Y. A new tool for diagnosing parathyroid lesions: angio plus ultrasound imaging. J Thorac Dis

2019;11:4829-34.
22. Adler DD, Carson PL, Rubin JM, Quinn-Reid D. Doppler ultrasound color flow imaging in the study of breast cancer: preliminary findings. Ultrasound Med Biol 1990;16:553-9.
23. Lloyd RV, Osamura RY, Kloeppel G, Rosai J. WHO classification of tumours of endocrine organs. 4th edition. Lyon: International Agency for Research on Cancer; 2017.
24. Esen G. Ultrasound of superficial lymph nodes. Eur J Radiol 2006;58:345-59.
25. Rettenbacher T. Sonography of peripheral lymph nodes part 1: normal findings and B-image criteria. Ultraschall Med 2010;31:344-62.
26. Ahuja AT, Ying M. Evaluation of cervical lymph node vascularity: a comparison of colour Doppler, power Doppler and 3-D power Doppler sonography. Ultrasound Med Biol 2004;30:1557-64.
27. Giovagnorio F, Galluzzo M, Andreoli C, De CM, David V. Color Doppler sonography in the evaluation of superficial lymphomatous lymph nodes. J Ultrasound Med 2002;21:403-8.
28. Rickes S, Sitzy J, Neye H, Ocran KW, Wermke W. High-resolution ultrasound in combination with colour-Doppler sonography for preoperative localization of parathyroid adenomas in patients with primary hyperparathyroidism. Ultraschall Med 2003;24:85-9.
29. Koslin DB, Adams J, Andersen P, Everts E, Cohen J. Preoperative evaluation of patients with primary hyperparathyroidism: role of high-resolution ultrasound. Laryngoscope 1997;107:1249-53.
30. Mazzeo S, Caramella D, Lencioni R, Viacava P, De Liperi A, Naccarato AG, Armillotta N, Marcocci C, Miccoli P, Bartolozzi C. Usefulness of echo-color Doppler in differentiating parathyroid lesions from other cervical masses. Eur Radiol 1997;7:90-5.
31. Mohammadi A, Moloudi F, Ghasemi-rad M. The role of colour Doppler ultrasonography in the preoperative localization of parathyroid adenomas. Endocr J 2012;59:375-82.
32. Park I, Rhu J, Woo JW, Choi JH, Kim JS, Kim JH. Preserving Parathyroid Gland Vasculature to Reduce Post-thyroidectomy Hypocalcemia. World J Surg 2016;40:1382-9.
33. Wang JB, Su R, Jin L, Zhou L, Jiang XF, Xiao GZ, Chu YY, Li FB, Feng YB, Xie L. The Clinical Significance of Detecting Blood Supply to the Inferior Parathyroid Gland Based on the "Layer of Thymus-Blood Vessel-Inferior Parathyroid Gland" Concept. Int J Endocrinol 2022;2022:6556252.
34. Shaari AL, Spaulding SL, Xing MH, Yue LE, Machado RA, Moubayed SP, Mundi N, Chai RL, Urken ML. The anatomical basis for preserving the blood supply to the parathyroids during thyroid surgery, and a review of current technologic advances. Am J Otolaryngol 2022;43:103161.
35. Jung HK, Park AY, Ko KH, Koh J. Comparison of the Diagnostic Performance of Power Doppler Ultrasound and a New Microvascular Doppler Ultrasound Technique (AngioPLUS) for Differentiating Benign and Malignant Breast Masses. J Ultrasound Med 2018;37:2689-98.

Cite this article as: Fang S, Zhu Q, Zhao J, Chang X, Liao Q, Wang O, Xing X, Li J, Liu H. Ultrasound diagnosis of parathyroid adenomas mimicking normal lymph nodes: microvascular clues. Quant Imaging Med Surg 2025;15(3):2222-2231. doi: 10.21037/qims-24-2057

